Thin-Walled Structures 49 (2011) 1017–1031

Contents lists available at ScienceDirect

Thin-Walled Structures

journal homepage: www.elsevier.com/locate/tws

Buckling and postbuckling behavior of unstiffened slender curved plates under uniform shear

Mozhdeh Amani [a], B.L.O. Edlund [b,*], M.M. Alinia [a]

[a] Department of Civil Engineering, Amirkabir University of Technology, Tehran, Iran
[b] Chalmers University of Technology, Civil and Environmental Engineering, Sven Hultins gata 8, SE-41296 Göteborg, Sweden

ARTICLE INFO

Article history:
Received 28 October 2010
Received in revised form
2 March 2011
Accepted 17 March 2011
Available online 19 April 2011

Keywords:
Curved plates
Shear
Buckling
Imperfection

ABSTRACT

Buckling and postbuckling behavior of curved plates under in-plane shear are investigated. After revisiting classic elastic buckling results, the elastoplastic postbuckling behavior and the effects of curvature parameter and aspect ratio are simulated via geometrical and material nonlinear analyses. Imperfection sensitivity is studied for various imperfection shapes and magnitudes. An increase in curvature parameter raises the elastic buckling load, produces unstable buckling and reduces postbuckling reserves. The buckling load and shear capacity are higher in shorter plates. Small initial imperfections are found to have severe effects on the initial buckling load of plates with large curvature parameter, but little effect on ultimate postbuckling capacity.

1. Introduction

Curved plates can be efficient force transmitters in structures. They are utilized in various civil engineering structures (e.g. web panels in horizontally curved steel plate and box girder bridges), as well as in aerospace, marine, and automotive applications.

Pure shear is a fundamental load case in plate and shell buckling problems, produced by direct shear or torsion. Therefore, due to the instability commonly associated with thin curved plates carrying such membrane stresses, their buckling and postbuckling behavior should be studied. Fig. 1 depicts the geometrical and loading properties of a cylindrically curved plate in pure shear considered in this research.

The buckling and postbuckling behavior of slender flat plates under shear has been well documented in the literature (see e.g. [1]). However, owing to the nonexistence of simple trigonometric shape functions for shear buckling modes of curved plates, it is more difficult to calculate their theoretical buckling loads [2]. An early analysis of the critical buckling behavior of a long, slightly curved plate under uniform shear stress was made by Leggett in 1937 [3]. The longitudinal edges were hinged (alternatively clamped) in a way that prevented the tangential displacements perpendicularly to these edges. Because the panel was very long, the boundary conditions at the curved edges were left undefined (ignored). In Germany, Kromm [4] published a paper in 1939 on this problem, but also treated panels with larger curvature parameters. The longitudinal edges were simply supported. Because tangential displacements normal to these edges were allowed to take place, the calculated buckling stresses became lower than those found by Leggett. The difference between the results of these two authors increases with the curvature parameter Z. In 1947, Batdorf et al. [5] found a fair trigonometric shape function for small deflection (bifurcation) buckling of cylindrically curved rectangular plates with simply supported edges. They theoretically solved the problem and computed curves for critical shear stresses of perfect panels. The results were in good agreement with those of Kromm.

Real curved plates are not perfect, but have some initial imperfections like deviations from nominal geometric parameters, load eccentricities or variations in material properties and other irregularities [6].

Nowadays, the deterministic design of shells and shell-like structures is essentially based on one of the following two approaches: (1) classical critical load (bifurcation) analysis combined with empirical knockdown factors [7], which represent lower bounds to the available experimental data or (2) numerical simulation by finite element analysis; cf. [8].

A basically different kind are the probability-based approaches, which may make use of a large imperfection data bank, where measured initial imperfections are defined by Fourier coefficients, see Arbocz et al. [9,10] and references therein.

In 1945, Koiter [11] developed a general theory for the initial postbuckling behavior of elastic systems with special reference to those with unstable postbuckling behavior. This asymptotic approach also gives a fair approximation of the reduced limit load

* Corresponding author. Tel.: +46 31470679; fax: +46 317722260.
E-mail address: bo.edlund@chalmers.se (B.L.O. Edlund).

0263-8231/$ - see front matter © 2011 Elsevier Ltd. All rights reserved.
doi:10.1016/j.tws.2011.03.007

Nomenclature

a	axial dimension of curved plate
a_{mn}	coefficients of deflection functions
b	circumferential dimension of curved plate
d	a or b, whichever smaller
D	flexural stiffness of plate per unit length
E	Young's modulus of elasticity
K_s	critical shear stress coefficient
r	curvature radius of plate
t	thickness of plate
u	displacement of median surface points of plate in axial (x) direction
v	displacement of median surface points of plate in circumferential (y) direction
V	applied shear force
V_y	shear yield load
w	displacement of median surface points of plate in radial direction; positive inward
w_0	amplitude of initial imperfections
x	axial coordinate of curved plate
y	circumferential coordinate of curved plate
Z	curvature parameter ($Z=(d^2/rt)\sqrt{1-\upsilon^2}$)
β	plate aspect ratio ($=a/b$)
υ	Poisson's ratio
ψ	relative shear buckling load for imperfect panel (compared with perfect case)
τ	applied shear stress
τ_{cr}	critical shear stress
τ_y	shear yield stress

due to small shape imperfections. Several numerical investigations were conducted to find the maximum supported load up to the onset of buckling, and to relate the buckling strength to the magnitude and form of initial imperfections [6,12,13]. An early theoretical study of the effect of initial imperfections on the buckling load was made by Donnell and Wan in 1950 [14], cf. also Koiter [15]. In addition, a large number of other numerical investigations [8,16,17] were conducted to find the minimum supported load in the postbuckling range.

On the other hand, the necessity to consider nonlinear behavior in shell buckling and postbuckling analysis has been recognized since long [1,18]. Modern FEA software together with powerful computer hardware enable the analysis of the load-carrying behavior of plates and shells accounting for both geometric and material nonlinearities plus initial imperfections.

Featherston [19] outlined a series of experiments carried out to determine the accuracy of analytical and FE techniques in predicting the buckling loads and postbuckling behavior of a simple aerofoil under combined shear and in-plane bending. It was emphasized that in carrying out a FE analysis many decisions must be made to select the various elements of the mathematical model; which requires a significant amount of experience and expertise from the designer in order to produce accurate results. To add on, validation by comparison with further data is necessary in order to have confidence in the results. It was further concluded that a combination of both methods should be used when designing components where buckling is a potential failure mode.

There are two main numerical approaches available for FE analysis of nonlinear structural response. They include static and dynamic analyses under slowly changing loads. The algorithms for static analysis often lead to convergence problems, as reported

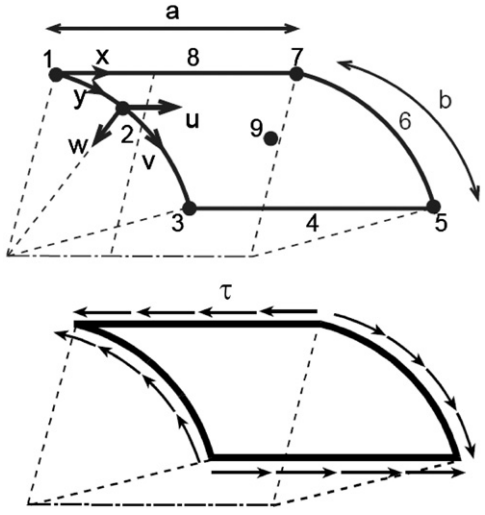

Fig. 1. General view of a curved plate loaded in shear.

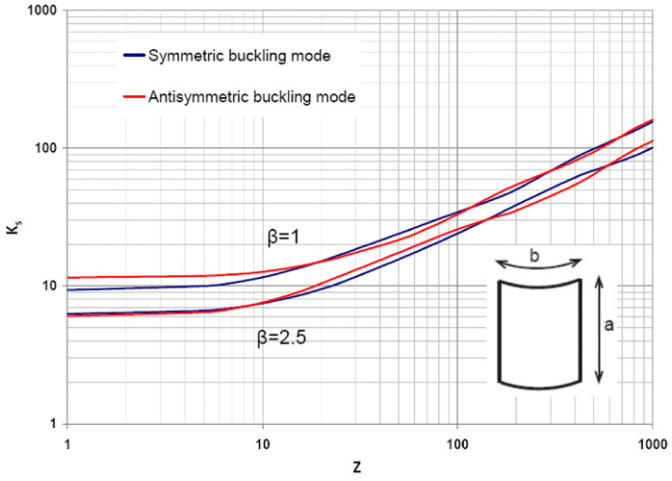

Fig. 2. Symmetric and antisymmetric elastic shear buckling coefficients of curved plates with different aspect ratios.

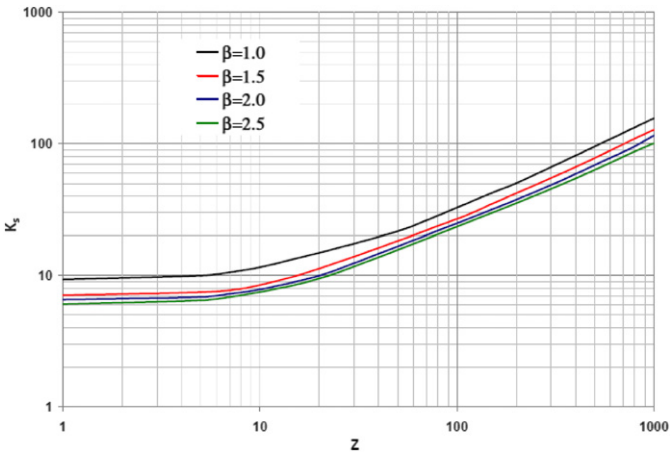

Fig. 3. Critical shear buckling coefficients of curved plates with $\beta \geq 1$.

by several researchers during recent years [20–24], and can cause obstacles when studying the behavior in the (advanced) post-buckling range. Convergence problems usually occur for shells due to clustering of bifurcation loads and unstable structural response through buckling [2]. Several approaches have been introduced to overcome difficulties in modeling such behavior. One approach is the use of "modified Riks' method". This method uses the load magnitude as an additional unknown; and solves simultaneously for loads and displacements. Thus, it has the merit of finding equilibrium states and provides solutions regardless of whether the response is stable or unstable. Another approach is to involve dynamic effects, taking account of inertia forces, when the structure snaps through. This objective is easily achieved via dynamic procedures under slowly changing loads (quasi-static loading) [2,18].

Small geometric imperfections can cause large reductions in buckling strength of shells [13,18]. This imperfection sensitivity is highly geometry/load dependent. Featherston [6] presented the effects of varying imperfection shape and amplitude on the buckling and postbuckling behavior of a curved panel under combined shear and compression. It was shown that the initial buckling load of curved panels under compressive loads is substantially reduced by the existence of imperfections, in particular geometric imperfections; and that it is essential to consider imperfections in analyzing such panels accurately. It is not a simple task to decide upon suitable "amplitude" and "shape" of geometric imperfections to use in a fully nonlinear analysis. According to the advice of some FE codes, using imperfections based on the first eigenmode together with the maximum anticipated amplitude value based on the consideration of fabrication procedures should ensure satisfactory results. Experience shows, however, that this is not always true [8].

Domb and Leigh [25] utilized a FE package to implement a nonlinear buckling analysis technique for the prediction of initial buckling in simply supported curved panels subjected to pure shear. They defined the buckling load either by a top-of-the-knee criterion or as the first maximum load. Their results were used to update and expand the NACA design curves, and showed that the degree of initial imperfection strongly influences the buckling load, especially for panels with intermediate and large values of the curvature parameter Z. The panels were thin-walled ($r/t=1000$) and relatively long ($a/b=4.0$). The shape of the initial imperfections was defined as a linear combination of the first four buckling modes found from a linear eigenvalue solution. It was also stated that the currently used NACA design curves are conservative when applied to panels in the "highly curved range", which actually means "for large values of b/t" (i.e. about 150–460), because all panels had $r/t=\text{constant}=1000$.

1.1. Outline of this paper

In Section 2 of the present study, NACA's [5] equilibrium equations of perfect simply supported cylindrically curved elastic rectangular plates (cylindrical panels) under pure shear are revisited and solved more accurately by incorporating more terms in the coefficient matrices; and the related curves for elastic critical shear coefficient K_s are replotted. In Section 3, first, a number of numerical finite element eigenvalue analyses are carried out and the results are compared to those of the classical theory. In the next step, nonlinear buckling and postbuckling analyses of some perfect, thin-walled steel curved plates under uniform shear stress are carried out via both explicit/dynamic and Riks' approach and the results are compared. It is shown that the behavior predicted using the explicit/dynamic analysis is not representative of what actually happens in a displacement-driven experiment, and therefore is not used further in this study. Based on these results and using Riks' method, the buckling and postbuckling behavior of perfect, curved elastoplastic slender plates and their relation to the curvature parameter and aspect ratio are discussed. Finally, imperfection sensitivity analysis for curved steel plates under uniform shear is carried out. In this regard, the effects of amplitudes and shape functions of initial imperfections on the buckling behavior of such curved plates are studied.

2. Bifurcation buckling of perfect, elastic curved plates

In this section, the classical NACA papers from 1947 on the elastic shear buckling of perfect curved plates [5,26] are briefly

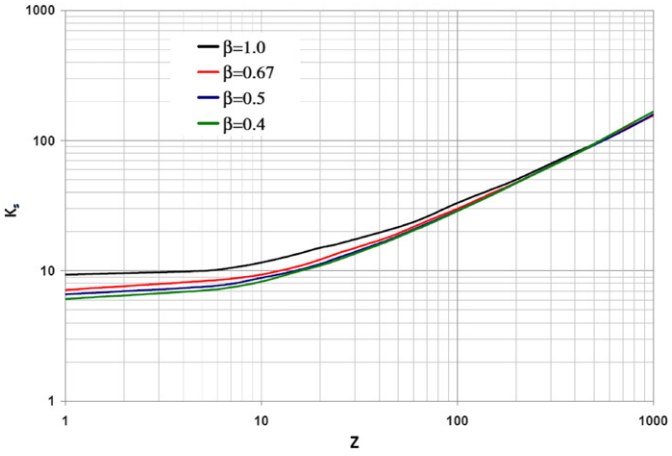

Fig. 4. Critical shear buckling coefficients of curved plates with $\beta \leq 1$.

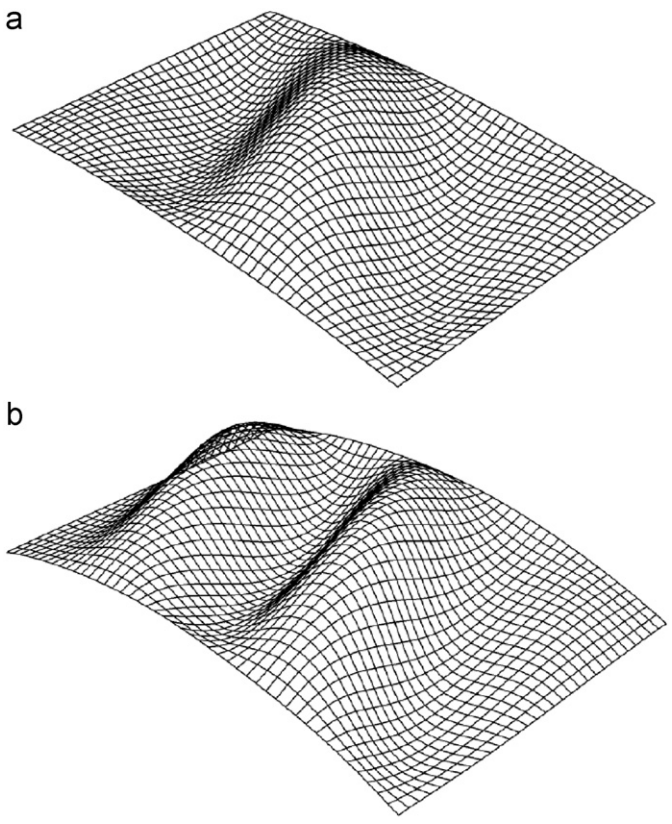

Fig. 5. Symmetrical (a) and antisymmetric (b) buckling mode shapes.

Table 1
Model characteristics.

Set	Model	$a \times b \times t$ (mm)	Z	β	Objective	Method
I	128 models	$1000 \times 1000 \times 3$ $1500 \times 1000 \times 3$ $2000 \times 1000 \times 3$ $2500 \times 1000 \times 3$	0–1000	0.40 0.50 0.67 1.00 1.50 2.00 2.50	To validate numerical procedure against theoretical results	Eigenbuckling analyses using Linear perturbation procedure
II	1	$1000 \times 1000 \times 3$	5	1.00	The buckling and postbuckling behavior of perfect curved plates under uniform shear	Fully nonlinear analyses using both Riks' and Dynamic/Explicit procedures
	2	$1000 \times 1000 \times 3$	15	1.00		Fully nonlinear analysis using Riks' procedure
	3		50		The effects of curvature parameter on the load-deformation response and yielding of perfect plates	
III	4	$1000 \times 1000 \times 3$	5		The effects of aspect ratio on the load-deformation response of perfect curved plates under shear	
	5		15			
	6		50			
	7		150			
	8	$1500 \times 1000 \times 3$	5	1.00		
	9		15			
	10		50			
	11		5			
	12		15	1.50		
	13		50			
	14	$2000 \times 1000 \times 3$	5	2.00		
	15		15			
	16		50			
	17	$2500 \times 1000 \times 3$	5	2.50		
	18		15			
	19		50			
	20	$1000 \times 2500 \times 3$	5	0.40		
	21		15		To compare the longer side being circumferential or axial on the behavior of perfect curved plates	
	22		50			
IV	23	$1000 \times 1000 \times 3$	5	1.00	The effects of initial imperfection *shape function* on the load-deformation response	Fully nonlinear analysis using Riks' procedure
	24		15			
	25		50			
	26	$2500 \times 1000 \times 3$	5	2.50		
	27		15			
	28		50			
	29	$1000 \times 1000 \times 3$	5	1.00		
	30		15		The effects of imperfection *amplitude* on the load-deformation response	
	31		50			
	32		150			
	33	$2500 \times 1000 \times 3$	5	2.50		
	34		15			
	35		50			

Table 2
Boundary conditions.

	u	v	w	θ_x	θ_y	θ_z
Corner 1	**1**	**1**	**1**	**0**	**0**	**0**
Edge 2	**0**	**0**	**1**	**0**	**0**	**0**
Corner 3	**1**	**0**	**1**	**0**	**0**	**0**
Edge 4	**0**	**0**	**1**	**0**	**0**	**0**
Corner 5	**1**	**0**	**1**	**0**	**0**	**0**
Edge 6	**0**	**0**	**1**	**0**	**0**	**0**
Corner 7	**1**	**0**	**1**	**0**	**0**	**0**
Edge 8	**0**	**0**	**1**	**0**	**0**	**0**

(**1**=**restrained; 0**=**free**).

revisited. The general shape of curved plates and the associated coordinate systems are illustrated in Fig. 1. Regarding the plate aspect ratios, curved plates may either have longer straight sides ($\beta = a/b \geq 1.0$) or longer circumferential sides ($\beta \leq 1.0$). The plates

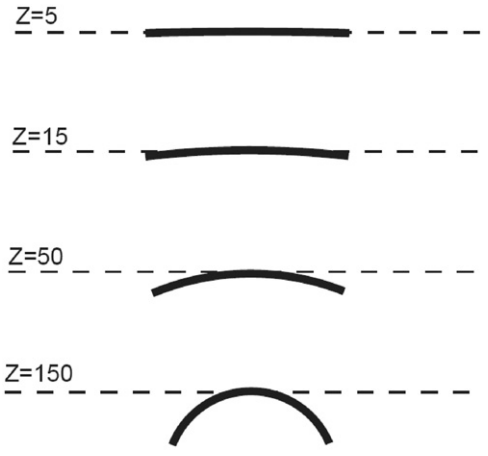

Fig. 6. Schematic views of plates with different curvature parameters.

are simply supported and loaded by uniform shear stresses along all four edges.

According to the NACA classical formulation by Batdorf et al. [5], the elastic shear buckling stress for cylindrically curved plates (cylindrical panels) is obtained from Eq. (1); where K_s is the elastic shear buckling coefficient which depends on the geometric parameters and boundary conditions and D is the flexural stiffness per unit length

$$\tau_{cr} = K_s \frac{\pi^2 D}{d^2 t}; \quad \text{where } d = a \text{ or } b, \text{ whichever smaller} \tag{1}$$

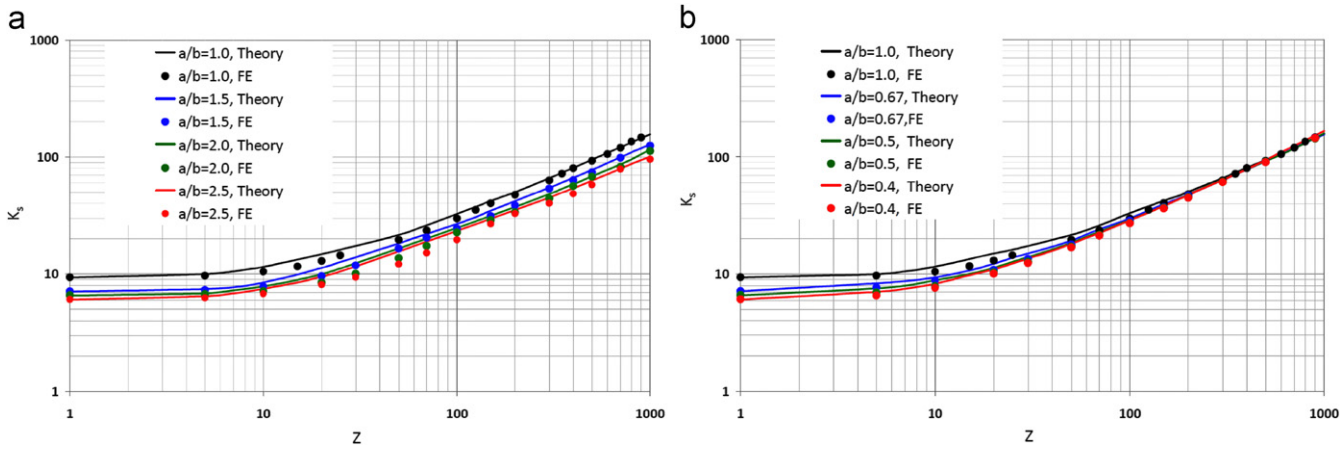

Fig. 7. Comparison between the "classic" NACA curves (Figs. 3 and 4) and the present FE analysis: (a) Plates with longer axial sides $\beta \geq 1$ and (b) Plates with longer curved sides $\beta \leq 1$.

Table 3
The first eigenmode shapes (via linear eigenbuckling analysis).

Z	$\beta=1$	$\beta=2.5$
5	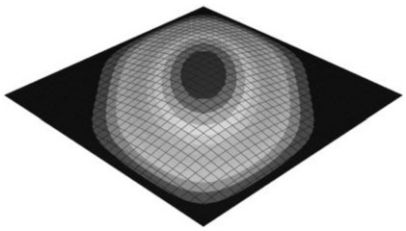	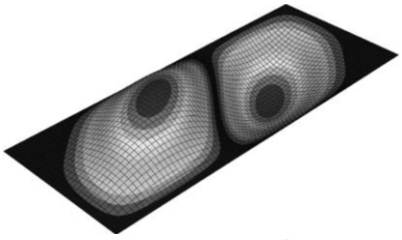
15	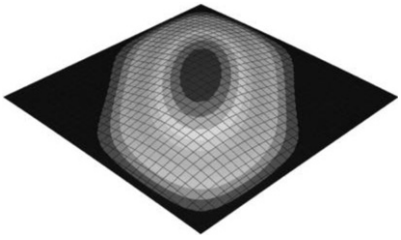	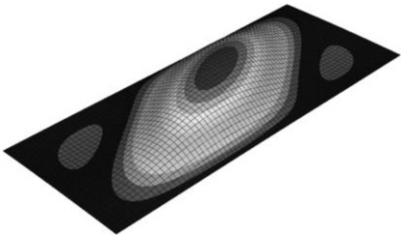
50	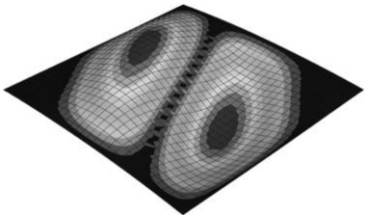	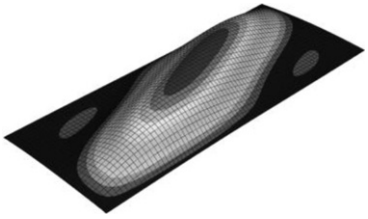
150	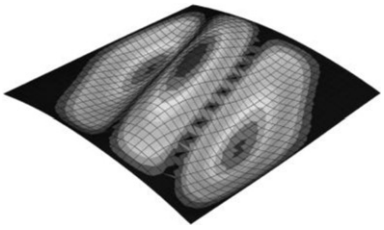	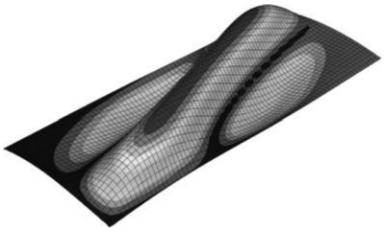

The equilibrium equation of a cylindrically curved rectangular plate was first established by Donnell [27] in 1933; and then modified by Batdorf [26] in 1947. Accordingly, the critical shear stress that causes a curved plate to buckle can be obtained by using Galerkin's method with the following differential equation:

$$D\nabla^4 w + \frac{Et}{r^2}\nabla^{-4}\frac{\partial^4 w}{\partial x^4} + 2\tau_{cr} t \frac{\partial^2 w}{\partial x \partial y} = 0 \quad (2)$$

For the solution, see further the Appendix. In the solution procedure, the software Mathematica [28] was used here to replot the NACA design curves.

Fig. 2 shows solutions for the case $\beta \geq 1.0$ for both symmetric and antisymmetric elastic buckling modes for simply supported curved plates having two different aspect ratios. Fig. 3 shows "cover" curves for plates with various aspect ratios, which represent the lowest of the two solution curves. The corresponding calculated curves for $\beta \leq 1.0$ representing the piecewise lowest of the two (symmetric and antisymmetric) elastic buckling coefficients are given in Fig. 4.

In general, the results imply that, depending upon the curvature parameter and aspect ratio, the buckling mode of curved plates under shear can be either symmetric or antisymmetric as shown in Fig. 5. The buckling curves presented in Fig. 3 indicate that the increase of curvature parameter causes alternating changes from symmetric to antisymmetric buckling modes. However, the style of this change is influenced by the plate's aspect ratio. In addition, in general for $\beta \geq 1.0$, the critical buckling stress of curved plates under pure shear is increased by the increase in curvature parameter and the reduction of aspect ratio (and for $\beta \leq 1.0$ the increase of aspect ratio).

3. Method of study and scope of the work

The objects for our FEA simulations are thin-walled steel panels with thickness 3 mm. The square panels and the shorter sides of the rectangular panels have side length 1 m. All the studied models are listed in Table 1.

The numerical analyses are performed by use of the finite element software package ABAQUS [29] and its S4R shell element. This four-noded quadrilateral doubly curved general-purpose shell element with reduced integration and a large-strain formulation, having five integration points through the thickness, is capable of showing shear strains. This type of shell element is consistent with thin shell theory and has three rotational and three translational degrees of freedom per node. Selecting a suitable mesh size leads to reasonably accurate results and efficient total CPU time. Based on a number of mesh sensitivity analyses, the element size of 33.33×33.33 mm^2 was selected as being the optimum choice in this study.

Structural steel was modeled as an elastic-perfectly plastic material, with the Young's modulus of elasticity $E = 200$ GPa and Poisson's ratio $= 0.3$. Von Mises' yield criterion and the associated flow rule was used in material plasticity; and the yield stress was presumed as 327.6 MPa according to ASTM A36 [30].

All edges of the curved plates, see Fig. 1, are presumed to be simply supported. The boundary conditions in the modeling procedure, which would ensure the state of pure shear, are given in Table 2. Shear forces are applied in the form of uniform shell edge loads along the middle surface of plates.

Four sets of analyses and results are presented in this paper. The first set is designed to validate the present numerical procedures against theoretical results. In the second set, Section 4.2, buckling and postbuckling behavior of initially perfect curved plates under shear is evaluated both with Riks' method and via quasi-static Dynamic/Explicit procedures. In the Dynamic/Explicit analyses, mass densities of shell elements are taken to be 7800 kg/m^3, and the loading rate is selected small enough to minimize the inertia effects. Viscous pressure loads of maximum magnitude 10 k Pa s/m

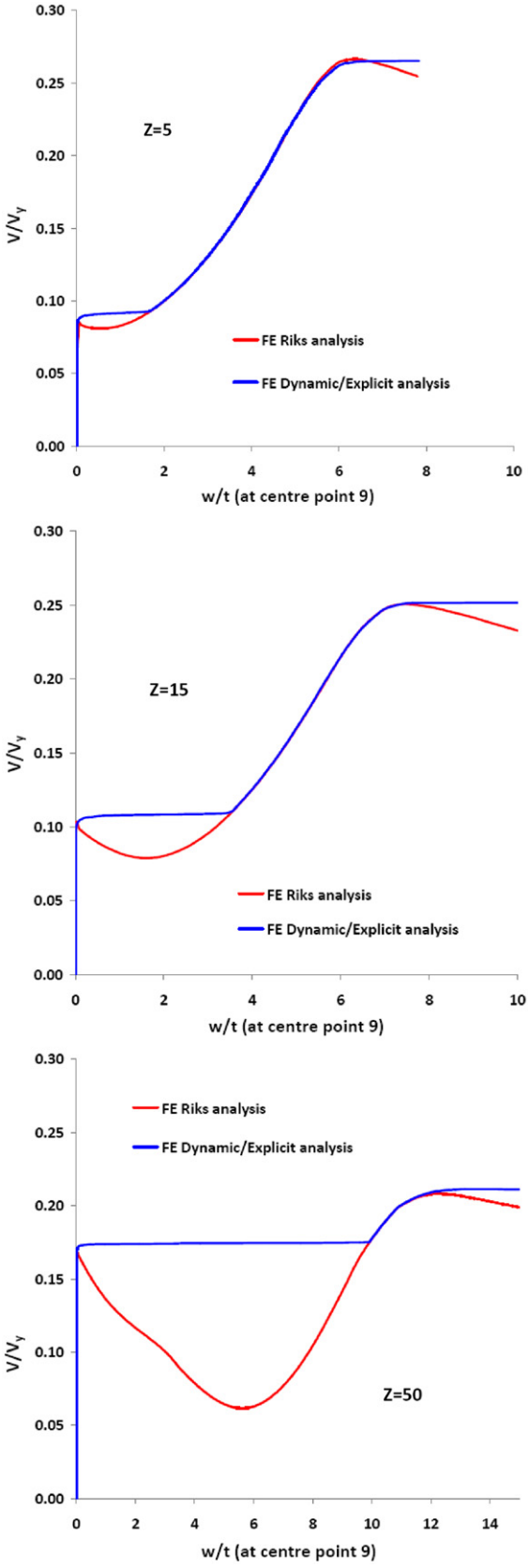

Fig. 8. Load–radial displacements of perfect curved plates.

are used to damp out the low-frequency dynamic effects (oscillations after snap-through).

In both approaches, primary linear eigenvalue analyses are first performed to determine the buckling mode shapes. This is then followed by nonlinear analyses where each panel is given very small initial radial deflections with the shape of the first eigenmode in order to initiate the buckling process. The analyses in the third and fourth sets use only Riks' method. They form a parametric study aimed at studying the effects of geometric parameters (curvature, aspect ratio and initial imperfections) on the load-displacement response of curved plates under shear. The characteristics of selected models are given in Table 1. Analysis set III concerns the effect of (a) curvature parameter, (b) aspect ratio ($\beta > 1.0$), and (c) aspect ratio ($\beta \leq 1.0$), for perfect curved plates. Set IV deals with the effect of initial imperfections with respect to their (a) shape and (b) amplitude. In order to visualize curvature parameters, the schematic shapes of selected curvature parameters are shown in Fig. 6.

4. Discussion of results

4.1. Validation of FE results—linear bifurcation buckling

The first set of analyses was designed to validate the numerical procedures against theoretical results previously described in Section 2. A variety of curved elastic perfect plates with wall thickness 3 mm, but different aspect ratios ranging from 0.4 to 2.5 in combination with different curvature parameters ranging from 0 to 1000, as stated in Table 1, was considered. The collected results obtained from this set of analyses are given in Fig. 7. The results from the linear eigenvalue analyses show that in geometrically perfect curved slender plates, the FE shear buckling coefficients are in conformity with those obtained from the classical formulas, and that the proposed NACA design curves can be used to predict elastic shear buckling loads of perfect curved plates. It is observed that the slight discrepancy between the theoretical and the FEA results becomes greater in plates having intermediate curvature parameter, which may be attributed to the alternating changes between symmetric and antisymmetric buckling modes (jumps) in the intermediate range between the small and highly curved plates.

For further illustration of this conformity, the first eigenmode shapes obtained via linear eigenbuckling analysis of plates having different curvature parameters and two typical aspect ratios are provided in Table 3. Cf. Fig. 2. It is observed that the number of buckling half waves in Table 3, which represents the symmetric or antisymmetric FE buckling mode shapes for the given curvature parameters and aspect ratios are in conformity with the theoretical lower curves for each case presented in Fig. 2.

4.2. Buckling and postbuckling behavior of perfect curved plates

The second set of analyses was designed to evaluate the buckling and postbuckling behavior of curved plates under shear. As mentioned earlier, several approaches have been introduced to overcome difficulties in modeling the unstable postbuckling behavior of shell structures. One approach is to use the modified

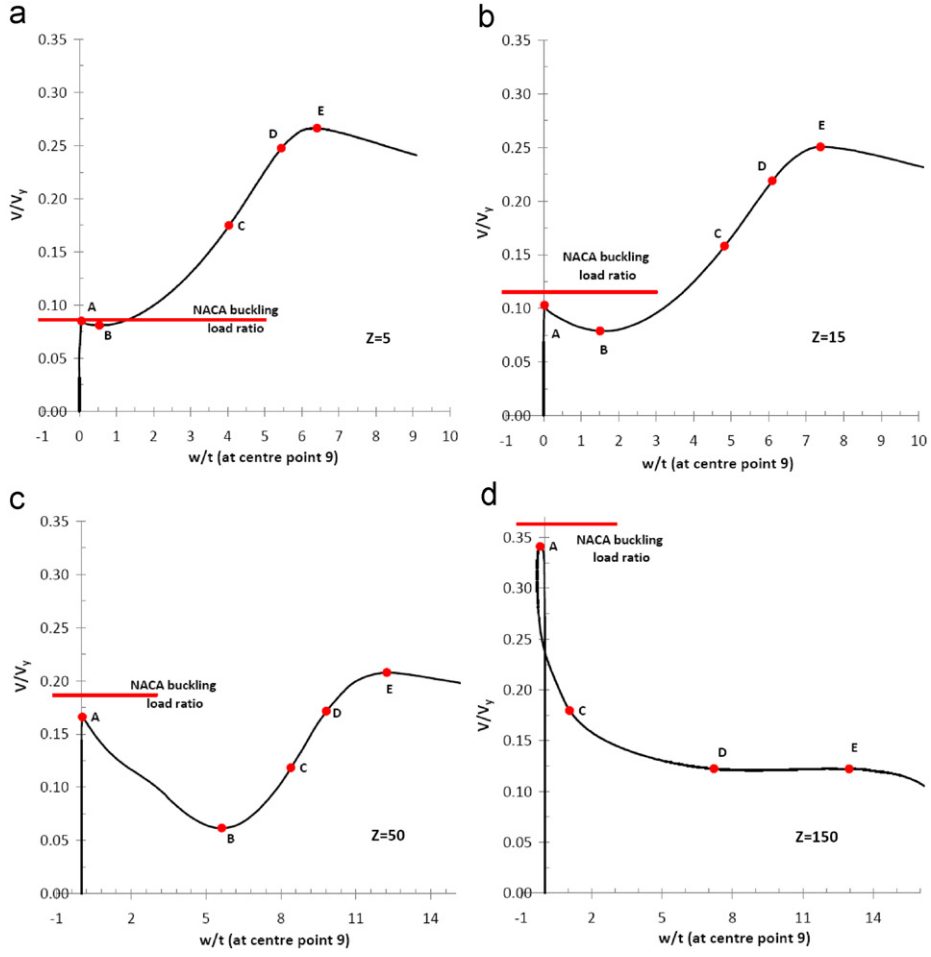

Fig. 9. Load–radial displacement diagrams: (a) model no. 4, (b) model no. 5, (c) model no. 6 and (d) model no. 7.

Riks' method, which is very useful in solving complex stability problems, typically at points where the equilibrium changes from stable to unstable, e.g. at a limit load. Another approach is to involve dynamic effects achieved via dynamic procedures under slowly changing loads (quasi-static loading). The load vs. radial displacement curves at the center (point 9 in Fig. 1) for three typical curved plates, see models 1–3 in Table 1, each formed from a square plate of dimensions $1000 \times 1000 \times 3\ mm^3$ obtained by the two FE approaches (ABAQUS Standard and Explicit) are plotted in Fig. 8. The values of the curvature parameter are $Z=5$, 15, and 50, respectively. In these diagrams, the results obtained via the FE Dynamic/Explicit analysis are compared to those obtained from the FE modified Riks' method.

Before the onset of buckling, the inertia forces are negligible and thus both the elastic pre-buckling response and the buckling loads obtained via both approaches are approximately identical. It is noted that by use of the dynamic analysis, the transient initial postbuckling behavior will be simulated. Thus, due to the effects of inertia forces, there is no "after-buckling load drop". On the other hand, in the static analysis, performed by Riks' arc-length method, equilibrium is established after each loading step. That method will therefore trace the initial postbuckling curve, which for curved plates is unstable and thus descending. After the first minimum level, the behavior along the rising curve is stable. Hence, the results from the two approaches in the first postbuckling phase are very different. However, beyond that postbuckling stage, the two curves converge and show a similar maximum capacity.

4.3. Parametric studies of perfect curved plates

The analyses worked out in the third set, see models 4–22 in Table 1, were aimed at studying the effects of geometric parameters on the load–displacement response of perfect curved plates under shear. These are static nonlinear analyses performed with Riks' method. The geometric parameters included curvature and aspect ratio. In the first part of this study, Section 4.3.1, four square plates having the dimensions $1000 \times 1000 \times 3\ mm^3$, but with different curvature parameter values ranging from 5 to 150 (models 4–7) were considered, cf. Figs. 9–11. Then plates with different curvature parameters and different aspect ratios ranging from 1.0 to 2.5 (models 8–19) were studied, Fig. 12. Finally, plates with the aspect ratio of 0.4 ($1000 \times 2500 \times 3\ mm^3$) and the curvature parameters of $Z=5$, 15, and 50 (models 20–22) were considered, and in Fig. 13 their buckling behavior is compared with that of the plates with $\beta=2.5$. In the presented load–displacement diagrams, the shear forces V and V_y are,

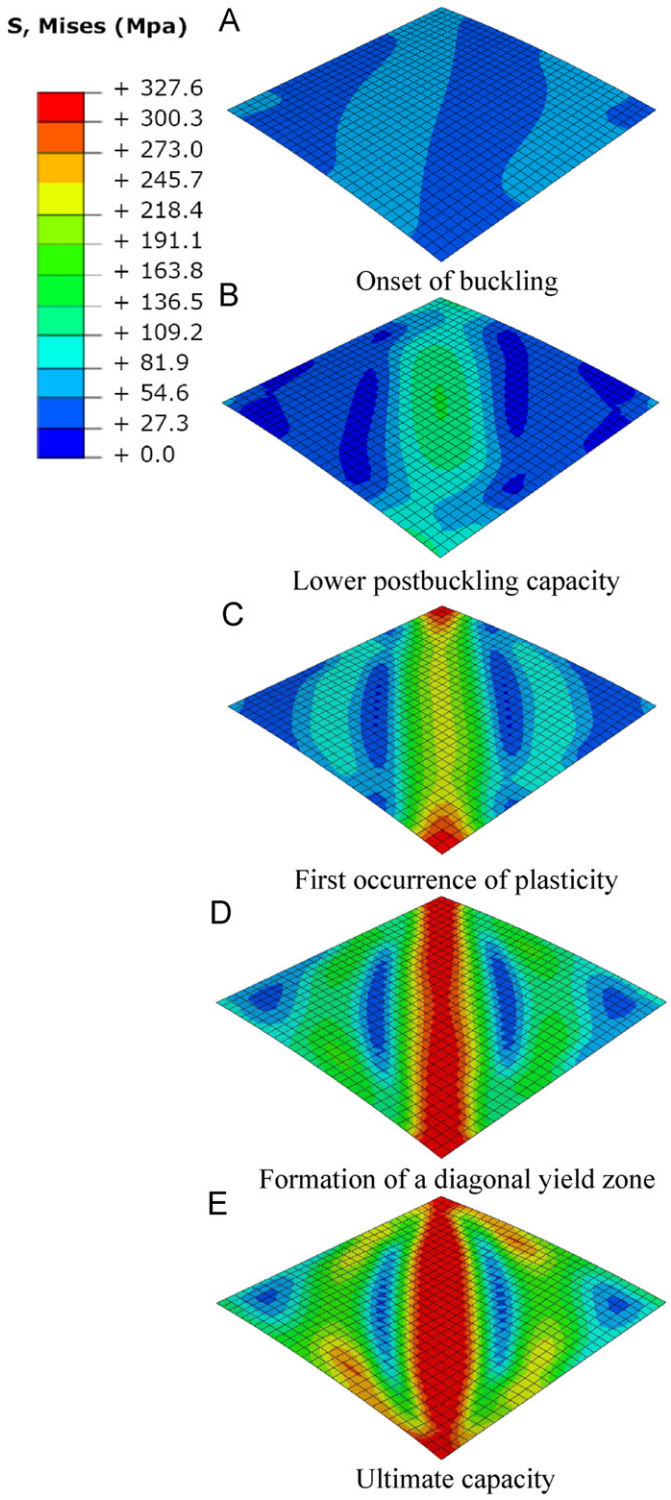

Fig. 10. Typical von Mises stress contours corresponding to stages defined in Fig. 9 for a square panel, $Z=50$.

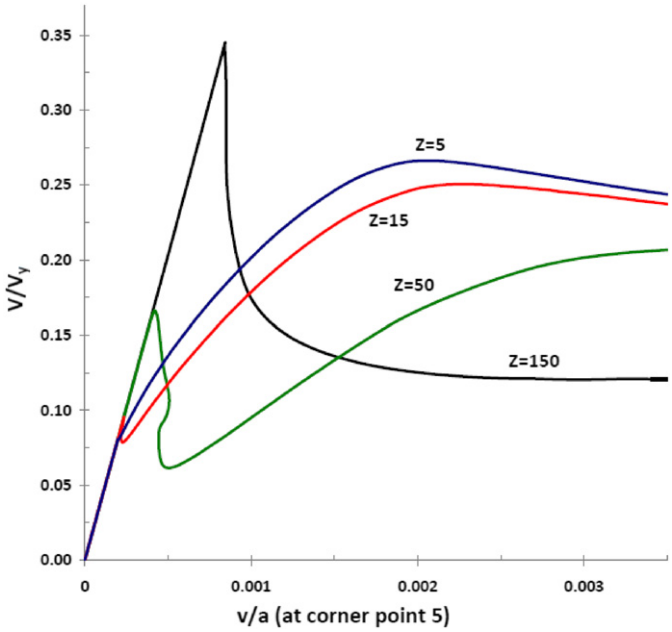

Fig. 11. Load–circumferential displacement diagrams of perfect square panels having various curvature parameters.

respectively, the applied load and the yield load. Noting that the magnitudes of V depend on the geometrical dimensions of the plate and V_y also on the material shear yield stress; and that they may be calculated by either of the following Eqs. (7a) or (7b) depending on the edge at which the applied load V is considered

$$V = at\,\tau \text{ and } V_y = at\,\tau_y \tag{7a}$$

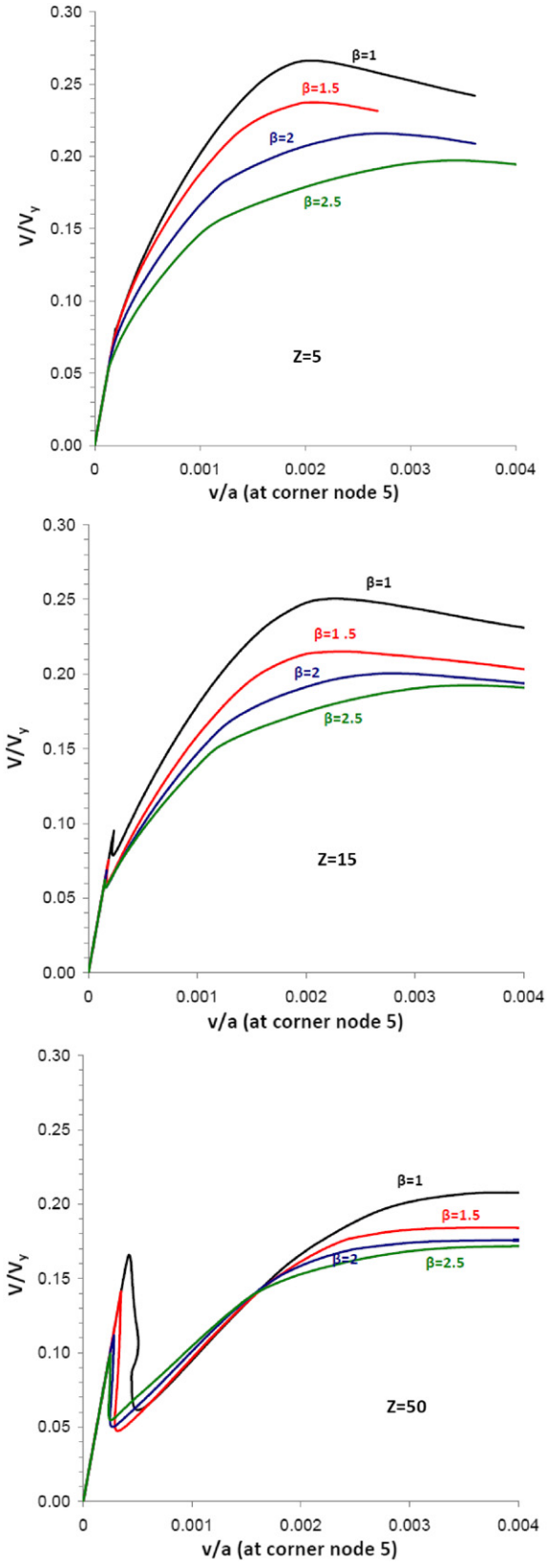

Fig. 12. Load–circumferential displacement of perfect curved plates with various curvatures and aspect ratios.

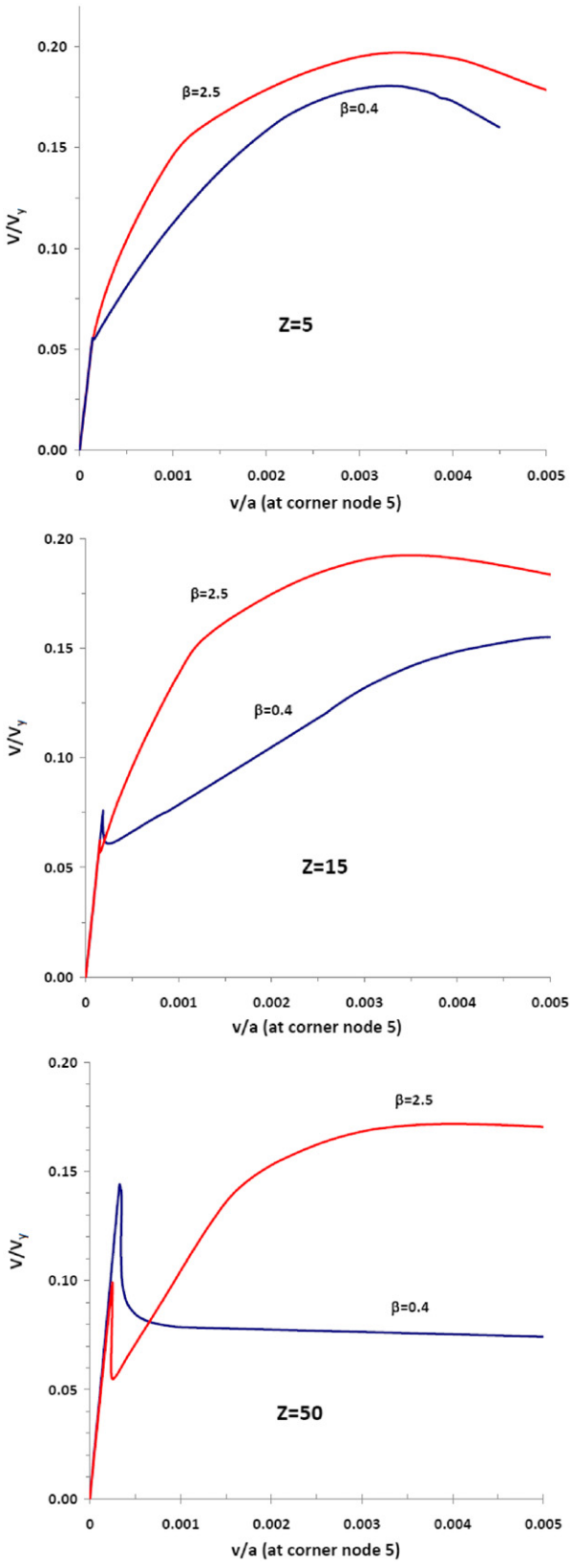

Fig. 13. Load–circumferential displacement of perfect curved plates having either axial or circumferential longer side and various curvatures.

$V = bt\tau$ and $V_y = bt\tau_y$ (7b)

Here τ is the applied shear stress; and the shear yield stress (τ_y) is defined by the von Mises yield criterion. It should also be noted that all simulations in analysis sets III and IV (Sections 4.3 and 4.4) were made with the modified Riks' method, which corresponds to performing physical experiments with displacement control.

4.3.1. *Influence of the curvature parameter Z*

The curves of load vs. radial displacement at the center (point 9 in Fig. 1) of four typical square plates are presented in Fig. 9. In these diagrams, point *A* corresponds to the onset of buckling; *B* to the minimum postbuckling load; *C* to the first material yielding; *D* to the formation of a diagonal yield zone; and *E* to what might be called "postbuckling strength" of curved plates.

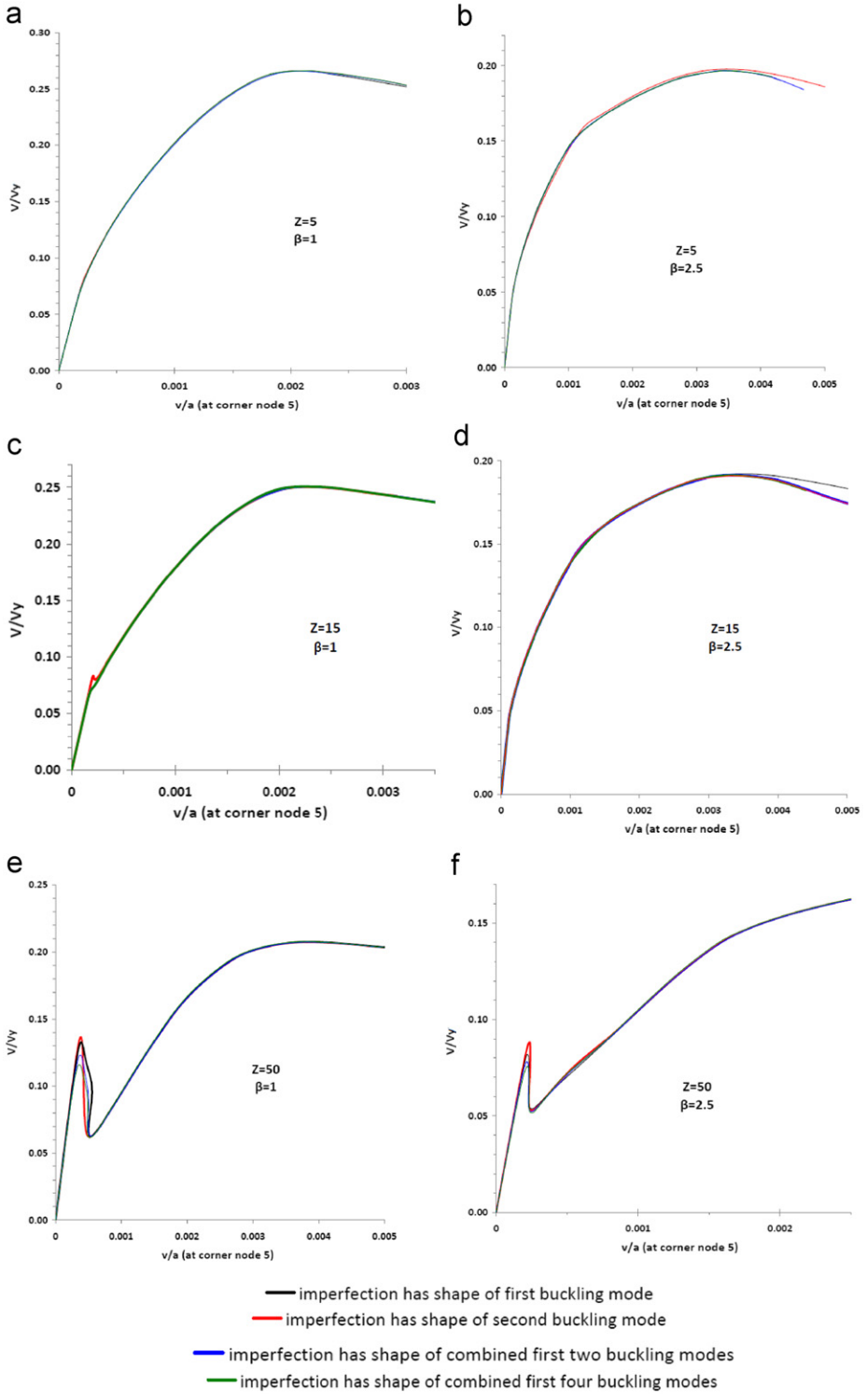

Fig. 14. Load–displacement curves of plates having imperfection amplitude $w_0 = 0.1t$ and various initial imperfection mode shapes.

Accordingly, the overall buckling/postbuckling behavior of curved steel plates can be divided into the following stages. OA is the linear elastic pre-buckling stage in which the in-plane shear force is proportionally increased up to the critical load, i.e. the bifurcation point. Immediately after the onset of buckling at point *A*, the equilibrium is unstable and a more or less sudden load reduction takes place. This load reduction is attributed to the exhaustion of membrane strength of curved plates due to the effects of buckling waves. The curve continues to descend until a new, stable geometric configuration at point *B* is formed. Therefore, AB is the initial postbuckling softening stage governed by geometric nonlinearities (which in load-controlled experiments may cause a "snap-through" phenomenon due to the plate curvature). The formation of the new, stable geometric configuration at point *B* enables the plate to carry further loads. Material yielding is then initiated at point *C* and continues to spread across the surface until the formation of a diagonal yield zone at point *D*; further on, a kind of "ultimate" capacity is reached at point *E*. Therefore, for moderately curved plates, the part BCDE may be referred to as the postbuckling hardening stage. Beyond point *E*, there is a second softening stage accompanied by large deformations and the spread of plasticity.

The von Mises stress contours corresponding to the aforementioned successive stages for a square curved plate with $Z=50$ are shown in Fig. 10. In addition, in Fig. 11 are depicted the four curves of the load vs. circumferential displacement relationship, i.e. V/V_y vs. v/a. Here v is measured at the corner point 5 (see Fig. 1) of the same plates as in Fig. 9.

In general, the results show that prior to the bifurcation phenomenon, the load-circumferential displacement response is almost linear and that the initial stiffness is not affected by the curvature parameter. By increasing the curvature parameter, the bifurcation buckling load increases. For plates with larger curvature parameter, however, there will in a displacement-controlled experiment be a load reduction (load "drop") immediately after buckling. The amount of this reduction increases with the curvature parameter.

In other words, when increasing the curvature parameter, the initial postbuckling response becomes more unstable. For some plates with large *Z*-values, it is noted, that there even occurs a so-called snap-back, i.e. in order to trace the descending curve it is also necessary to reduce the corner displacement v. In the advanced postbuckling range, the capacity is strongly reduced for plates with larger curvature parameter like $Z=150$, cf. Fig. 11.

On the other hand, plates with a small curvature parameter show a more "plate-like" behavior, having stable initial buckling response and a significant postbuckling reserve. The buckling response of plates with moderate curvature parameter is characterized by a relatively short, unstable early postbuckling range and then a considerable capacity in the advanced postbuckling range. As seen in Fig. 8 for a load-controlled process, the increase in curvature parameter can lead to a more pronounced snap-through behavior at buckling and smaller postbuckling reserves. For plates with very high curvature parameter, cf. model 7 ($Z=150$) in Fig. 9(d) and Fig. 11, there is no postbuckling reserve.

4.3.2. *Influence of the aspect ratio* β

Models 8–19 (see Table 1) were analyzed in order to evaluate the influence of aspect ratio on the buckling and postbuckling behavior of curved plates. The results obtained from the nonlinear FE analysis are given in Fig. 12. These diagrams are presented in the form of the relative applied shear load against the relative circumferential displacement (drift angle) v/a, where v is measured at the corner node 5.

The results show that the "initial circumferential stiffness" is not affected by the plate aspect ratio. On the other hand, for $Z=5$ and 15 longer curved plates reach lower relative loads at buckling and at maximum strength. For $Z=50$ that conclusion holds, although in the first part of the postbuckling range the situation is somewhat different.

The longer side of curved plates can be either axial or circumferential. Fig. 13 illustrates the difference in buckling and postbuckling behavior between models 20–22 (with $\beta<1$) and models 17–19 (with $\beta>1$), as defined in Table 1. It is observed, that in plates with longer circumferential sides, the relative bifurcation buckling loads are higher than for plates with longer axial sides ($\beta>1$). In plates with $\beta=0.4$, the curvature parameter effect is more pronounced and gives more efficient membrane action in the pre-buckling stage. At the initial buckling stage,

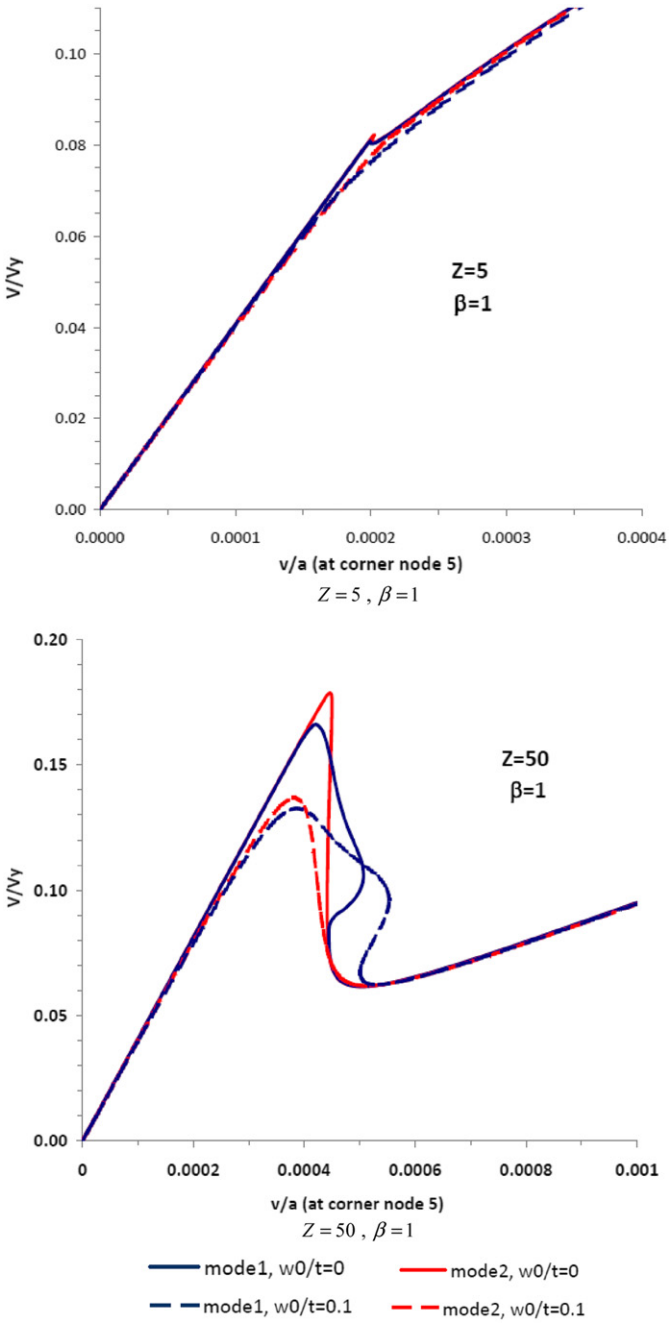

Fig. 15. Comparisons between perfect and imperfect cases for two typical curved panels ($Z=5$ and $Z=50$) ; cf. Fig. 14(a) and (e) (imperfect cases).

however, the disturbing effects of buckling waves lead to a larger drop in the relative load (than for plates with $\beta > 1$). Further, the postbuckling capacity is smaller.

4.4. Buckling behavior of imperfect curved plates

In the final set of analyses, models 23–35 (see Table 1) were utilized to inspect the effect of initial imperfections on the buckling strength and postbuckling behavior of curved plates under shear. The first group (i.e. models 23–28) was analyzed to consider the effects of the shape of initial imperfection (shape function) on the load-displacement response. Curved plates having various curvature parameters in combination with different aspect ratios, and having initial imperfections based on the first, the second, the combination of the first two and the combination of the first four eigenmodes were considered. The maximum imperfection amplitude in each case was given a constant value equal to 0.1 times the plate thickness. The second group (i.e. models 29–35) of analyses was performed to consider the effect of imperfection amplitude on the buckling strength and post-buckling behavior of curved plates. Finally, in this section, typical relationships between the imperfection amplitude and the "strength reduction" are compared.

4.4.1. Influence of the initial imperfection mode shape

The diagrams in Fig. 14 represent the variation of applied load against circumferential displacements measured at the corner point 5 of models 23–28. The results show that the assumption, that an imperfection of the shape of the first eigenmode often results in the most critical case, seems to hold for the lower range of Z-values. For larger Z-values, however, combined or higher

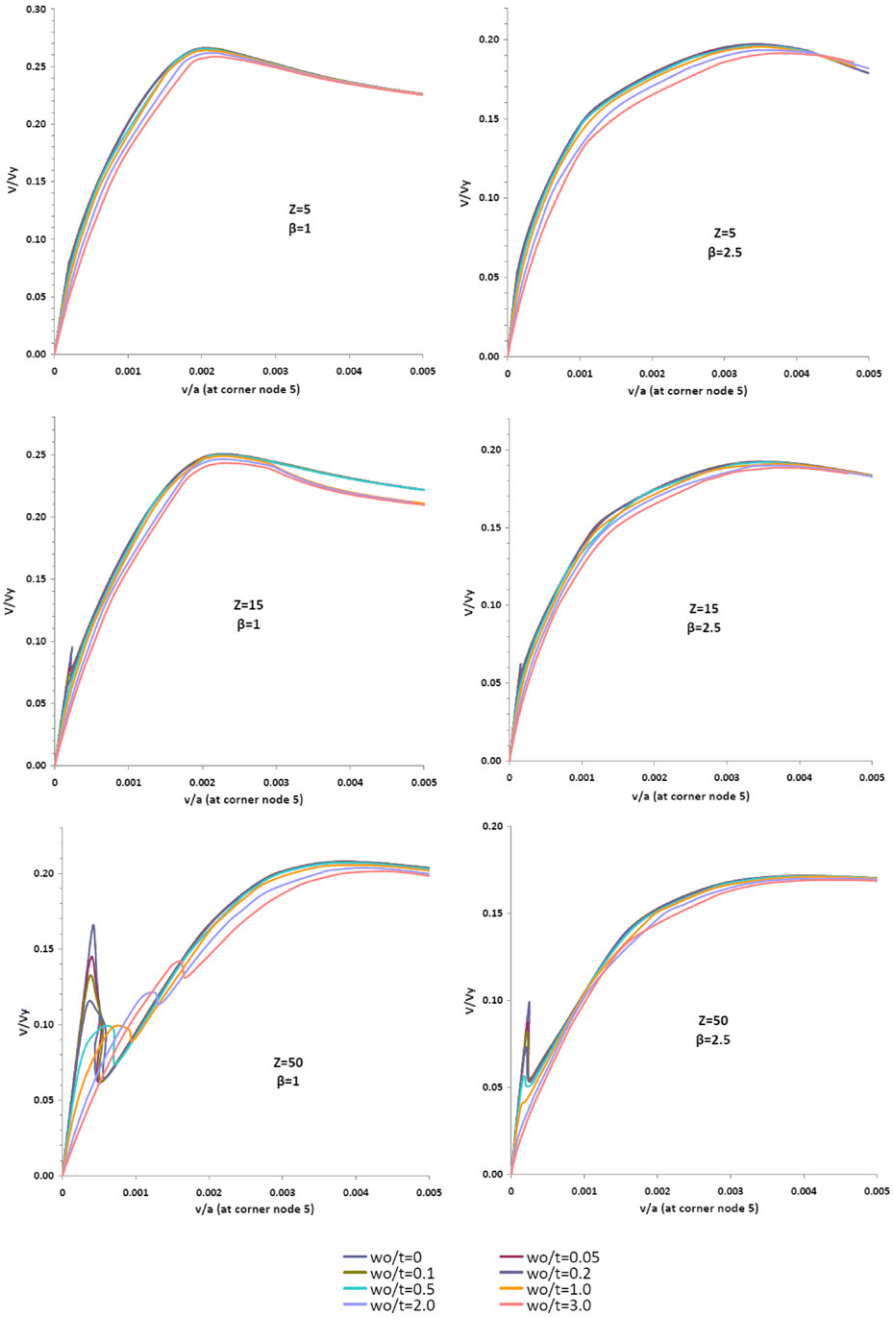

Fig. 16. Load–circumferential displacement of curved plates with initial imperfections based on first buckling mode and various amplitudes.

eigenmodes seem to result in somewhat lower buckling loads, cf. Fig. 14(e) and (f).

In Fig. 15 the buckling loads for the perfect and imperfect cases of two typical square curved panels ($Z=5$ and $Z=50$) are compared. The results show, among others, that the effect of initial imperfections on the initial buckling increases with the curvature parameter.

4.4.2. *Influence of the initial imperfection amplitude*

Figs. 16 and 17 show the results of analysis of models 29–35 and represent the effect of imperfection amplitude upon the buckling behavior of curved plates. The diagrams in Fig. 16 show the relative applied load against the relative circumferential displacement measured at the corner point 5 (see Fig. 1) of models 29–31 and 33–35. The imperfection shape is that of the first eigenmode. In the diagrams of Fig. 17 the deformations are represented by the relative radial displacements for models 31, 35, and 32 measured at the center point 9. (Note that the results for $Z=50$ in Figs. 16 and 17 are for the same models 31 and 35.)

The results show that by increasing the imperfection amplitude, the buckling load and the related "top-of-the- knee" in the load–circumferential displacement curves decrease. However, when the magnitude of initial imperfection becomes relatively large ($w_0/t \geq 1$), the bending and buckling displacements combine, and it will be less meaningful to try to use such curves to evaluate some quantity related to critical loads. Nevertheless, the postbuckling reserves and the ultimate capacities are practically not affected by the small and moderate initial imperfection magnitudes represented in Figs. 16 and 17.

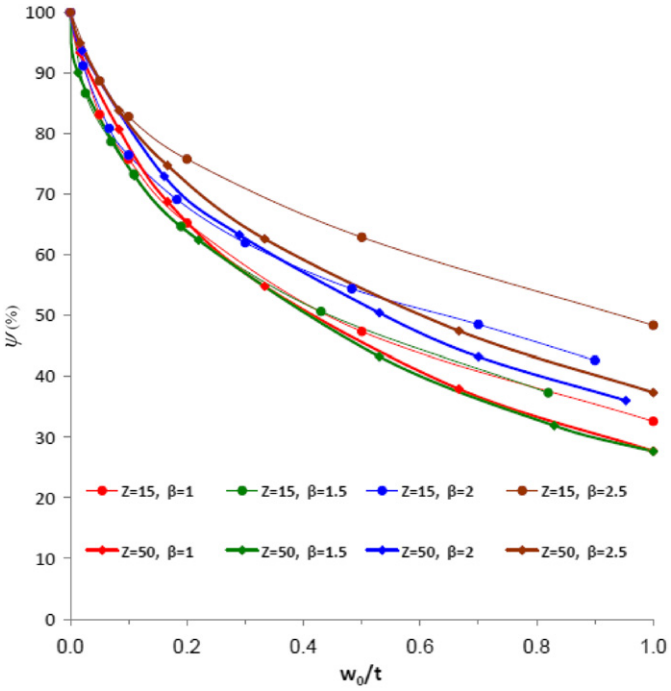

Fig. 18. Relative shear buckling load vs. initial imperfection amplitudes for panels with $Z=15$ and $Z=50$ and four aspect ratios. For perfect panels $\psi=100\%$. (N.B. In cases where clear bifurcation points were not detected, the related 'top-of-the-knee' load is presumed as the buckling load).

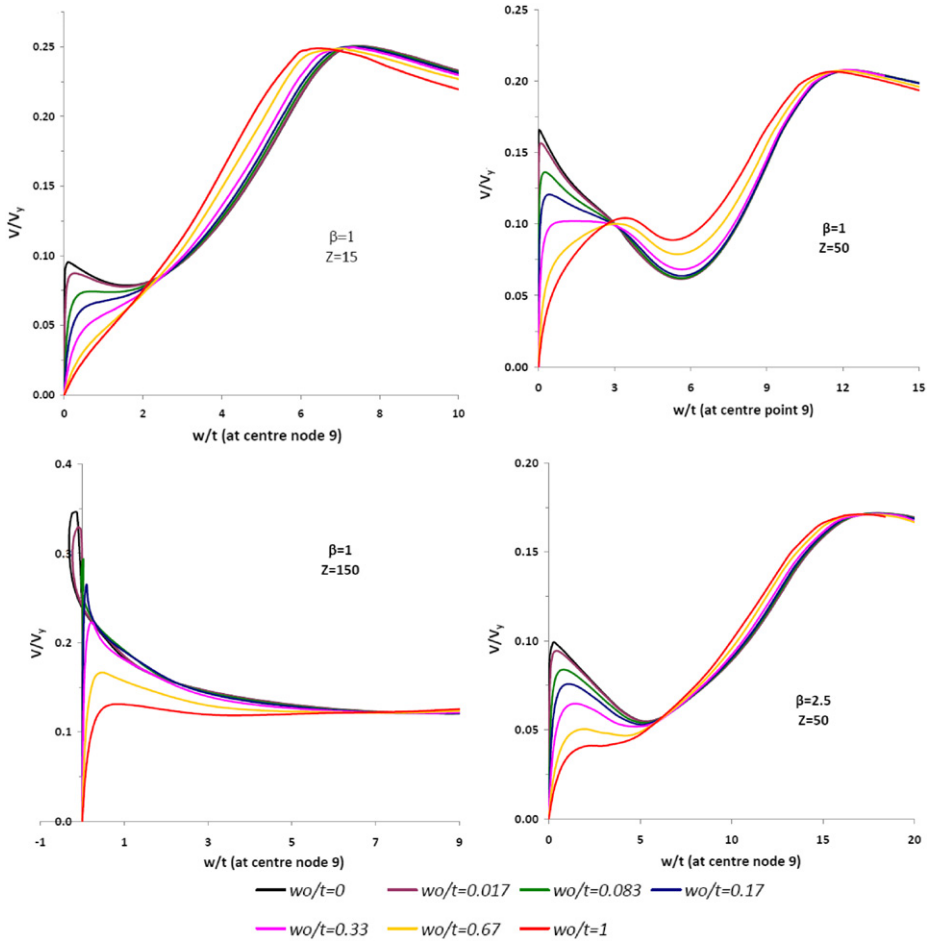

Fig. 17. Load–radial displacement of curved plates with initial imperfections based on first buckling mode and various amplitudes.

Finally in this paper, Fig. 18 is an illustration of the imperfection sensitivity for various slender, curved plates. It represents a summary of results in the form of the percentage reduction in shear buckling load of imperfect plates vs. the relative initial imperfection amplitude for typical curved plates of $Z=15$ and $Z=50$ having various aspect ratios. It is noted that since initial imperfections can cause large reduction of classic buckling loads, they should be included in the design procedures. The figure indicates that the effect of initial imperfections, see Figs. 14–18, is more pronounced in plates with larger curvature parameter Z and smaller aspect ratio a/b (>1).

5. Conclusions

The following conclusions are drawn from the aforementioned investigations on the buckling and postbuckling behavior of perfect and imperfect thin curved plates subjected to uniform in-plane shear forces:

- The NACA classic shear buckling design curves for cylindrical panels are only correct in predicting the elastic buckling load of perfect shallow curved plates. The degree of curvature and the existence of initial imperfections can cause significant deviations from the classic formula results.
- The two fully nonlinear FE approaches, i.e. the modified Riks' method and the Dynamic/Explicit procedure, may both be utilized to predict the critical load and the ultimate capacity of curved plates. These methods, however, can be used in a complementary manner to get a more complete picture of the postbuckling characteristics of such elements.
- Prior to the bifurcation load, the load–displacement response of a perfect panel is almost linear and the initial circumferential stiffness is affected neither by curvature parameter nor by the aspect ratio.
- By increasing the curvature parameter, the shear buckling load increases. However, under displacement control, this increase is followed by a load drop immediately after buckling. The amount of this load reduction increases with the curvature parameter. In addition, the increase in curvature parameter produces a more unstable initial buckling response.
- Plates with small curvature parameters have more stable initial buckling behavior followed by significant postbuckling reserves. The buckling response of moderately curved plates is slightly unstable with subsequent considerable postbuckling capacities. In more curved plates, there is only a small postbuckling reserve. In plates with very large curvature parameter, there is no postbuckling stage with load increase due to the highly unstable buckling response.
- Plates with longer circumferential sides have higher relative buckling loads than comparable panels with longer axial sides. On the other hand, their initial buckling responses are more unstable and the relative ultimate load is smaller. Longer curved plates have lower relative buckling load and ultimate load than the shorter and square plates.
- The effect of initial imperfections on the buckling behavior of curved plates increases with the curvature parameter. In dealing with initial imperfection shape functions for low curvature panels (small Z), it is sufficient to consider the first eigenmode shape. For plates with larger Z-values, however, there might be lower buckling loads when imperfections are based on combined higher eigenmodes, e.g. combinations of the first two or first four modes.
- When increasing the amplitude of small initial imperfections, the shear buckling load of curved plates decreases, but their postbuckling response remains practically unchanged.
- Initial imperfections can considerably reduce the shear buckling capacity. This effect is more significant in plates having larger curvature parameters and smaller aspect ratios.

Appendix A. Determination of the buckling coefficient for shear K_s

The basis is the differential Eq. (2). Galerkin's method is used to calculate K_s. For simply supported curved rectangular plates with axial sides longer than circumferential sides ($\beta \geq 1.0$), the radial displacement function is presumed as

$$w=\sum_{m=1}^{\infty}\sum_{n=1}^{\infty} a_{mn}\sin\frac{m\pi x}{a}\sin\frac{n\pi y}{b} \tag{A1}$$

m and n are the number of buckling half waves in the axial and circumferential directions, respectively. According to Galerkin method the coefficients a_{mn}, are chosen to satisfy the following equation:

$$\int_0^a\int_0^b \sin\frac{p\pi x}{a}\sin\frac{q\pi y}{b}\left(\nabla^4 w+\frac{12Z^2}{b^4}\nabla^{-4}\frac{\partial^4 w}{\partial x^4}+2K_s\frac{\pi^2}{b^2}\frac{\partial^2 w}{\partial x\partial y}\right)dxdy=0$$

$$p,q=1,2,3,\cdots \tag{A2}$$

where Z is the curvature parameter defined by

$$Z=\frac{d^2}{rt}\sqrt{1-\upsilon^2};\ \text{where } d=a \text{ or } b, \text{whichever smaller} \tag{A3}$$

By substituting Eqs. (A1) into (A2), a set of homogenous linear algebraic equations is obtained as

$$a_{pq}\left[(p^2+q^2\beta^2)^2+\frac{12\beta^4p^4Z^2}{\pi^4(p^2+q^2\beta^2)^2}\right]+\frac{32\beta^3K_s}{\pi^2}\sum_{m=1}^{\infty}\sum_{n=1}^{\infty}a_{mn}\frac{mnpq}{(m^2-p^2)(n^2-q^2)}=0 \tag{A4}$$

Then by allocating different values for m and n, two sets of equations, which corresponds to symmetric and antisymmetric buckling modes are established via matrix coefficients given in the Appendices of Ref. [5]. The critical shear stress for a curved plate with the particular values of β and Z is found via minimizing the values of K_s for which the two sets of equations have a non-vanishing solution. The corresponding matrix coefficients for plates with longer curved sides ($\beta \leq 1.0$) are also given in the Appendices of Ref. [5].

The above-mentioned solution procedure is solved by Mathematica software [28] and the NACA design curves are replotted, see Figs. 2 and 3.

Appendix B. Supplementary material

Supplementary data associated with this article can be found in the online version at doi:10.1016/j.tws.2011.03.007.

References

[1] Alinia MM, Habashi HR, Khorram A. Nonlinearity in the postbuckling behavior of thin steel shear panels. Thin-Walled Struct 2009;47:412–20.
[2] Schneider W, Ribakov Y. Collapse analysis of thin walled cylindrical steel shells subjected to constant shear stress. Comput Struct 2004;82:2463–70.
[3] Leggett DMA. The elastic stability of a long and slightly bent plate under uniform shear. In: Proceedings of the Royal Society; 1937. A162, p. 62–83.
[4] Kromm A. The limit of stability of a curved plate strip under shear and axial stresses. NACA TM 898; June 1939.
[5] Batdorf SB, Stein M, Schildcrout M. Shear Stress of curved rectangular panels, NACA TN No. 1348; 1947.

[6] Featherston CA. Imperfection sensitivity of curved panels under combined compression and shear. J Non-Linear Mech 2003;38:225–38.
[7] Nemeth MP, Starnes JH. Jr, The NASA monographs on shell stability design recommendations, a review and suggested improvements, NASA TP 206290; 1998.
[8] Wang H, Croll J. Optimization of shell buckling using lower bound capacities. Thin-Walled Struct 2008;46:1011–20.
[9] Arbocz J. The imperfection data bank, a mean to obtain realistic buckling loads. In: Ramm E, editor. Buckling of Shells. Berlin: Springer-Verlag; 1982. p. 535–67.
[10] Arbocz J, Starnes Jr JH. Future directions and challenges in shell stability analysis. Thin-Walled Struct 2002;40:729–54.
[11] Koiter WT. On the stability of elastic equilibrium. PhD thesis, University of Delft; 1945.
[12] Hutchinson JW, Koiter WT. Postbuckling theory. Appl Mech Rev 1970;23: 1353–66.
[13] Hong T, Teng JG. Imperfection sensitivity and postbuckling analysis of elastic shells of revolution. Thin-Walled Struct 2008;46:1338–50.
[14] Donnell LH, Wan CC. Effect of imperfections on buckling of thin cylinders and columns under axial compression. J Appl Mech (ASME) 1950;17:73–83.
[15] Koiter WT. Current trends in theory of buckling. In: Budiansky B, editor. Buckling of structures. Berlin, Heidelberg, New York, Cambridge/US: Springer-Verlag; 1976. p. 1–6.
[16] Croll JGA, Batista RC. Explicit lower bounds for the buckling of axially loaded cylinders. Int J Mech Sci 1981;23(6):331–43.
[17] Kröplin B, Dinkler D, Hillmann J. An energy perturbation applied to nonlinear structural analysis. Comput Methods Appl Mech Eng 1985;52(1–3):885–97.
[18] Edlund BLO. Buckling of metallic shells: buckling and postbuckling behavior of isotropic shells, especially cylinders, Struct. Control Health Monit 2007;14: 693–713.
[19] Featherston CA. Experimental buckling of a simple aerofoil under combined shear and in-plane bending. Proc Inst Mech Eng Part C: J Mech Eng Sci 2004;218:155–72.
[20] Riks E, Rankin CC, Brogan FA. On the solution of mode jumping phenomena in thin-walled shell structures. Comput Meth Appl Mech Eng 1996;136:59–92.
[21] Hilburger MW, Waas AM, Starnes JH. Modeling the dynamic response and establishing postbuckling/post snap-thru equilibrium of discrete structures via a transient analysis. Trans ASME 1997;64:590–5.
[22] Choong KK, Ramm E. Simulation of buckling process of shells by using the finite element method. Thin Walled Struct 1998;31:39–72.
[23] Schneider W, Thiele R. Evaluation of failure states by means of a quasi-static analysis. Bauingenieur 1999;74:485–94.
[24] Schweizerhof K, Vielsack P, Rottner T, Ewert E. Stability and sensitivity investigations of thin-walled shell structures using transient finite element analysis, In: Proc 5th world congress on computational mechanics-WCCM V, Vienna; 2002, 〈www.wccm.tuwien.ac.at/publications/Papers/fp81329.pdf〉.
[25] Domb MM, Leigh BR. Refined design curves for shear buckling of curved panels using nonlinear finite element analysis. In: Proceedings of the 43rd AIAA/ASME/ASCE/AHS/ASC structures, structural dynamics, and materials conference, Denver, Colorado; 2002. AIAA preprint, p. 1257–66.
[26] Batdorf SB. A simplified method of elastic-stability analysis for thin cylindrical shells, II—Modified equilibrium equation, NACA TN No. 1342; 1947.
[27] Donnell L.H., Stability of thin-walled tubes under torsion, NACA Rep. No. 479; 1933.
[28] Wolfram Mathematica 6.0, Copyright 1988–2007 Wolfram Research Inc.
[29] ABAQUS 6.7-1 reference manual, ABAQUS Inc.
[30] ASTM Standards A36M, "Specification for Carbon Structural Steel", ASTM International, West Conshohocken, PA; 2005, doi:10.1520/A0036_A0036M-08, 〈www.astm.org〉.